Accurately Mapping Soil Profiles: Sensor Probe Measurements at Dense Spatial Scales

Tyler J. Lund, Eric D. Lund, Chase R. Maxton

Veris Technologies, Inc. USA

A paper from the Proceedings of the
16th International Conference on Precision Agriculture
21-24 July 2024
Manhattan, Kansas, United States

Keywords. soil, sensors, profile, horizons, carbon, health, compaction, moisture

Abstract
Proximal sensing of soil properties has typically been accomplished using various sensor platforms deployed in a continuous sensing mode collecting data along transects, typically spaced 10-20 meters apart. This type of sensing can provide detailed maps of the X-Y soil variability and some sensors provide an indication of soil properties within the profile, however without additional investigations the profile is not delineated precisely. Alternatively, soil sensor probes can provide detailed profile information with depth, however they have not been configured for high through-put and with multiple sensors for rapid, detailed mapping of field soil profiles. A new 0-60 cm CoreScan™ probe has been developed by Veris Technologies with Vis-NIR optical, soil EC, moisture, and force sensors and is configured to generate insertions at a dense spatial scale, typically .4 ha/insertion or less. The close insertion spacing allows more reliable interpolation of the data, and calibration with 0-60 cm soil cores results in 3D maps of soil properties such as clay content, organic carbon, compaction and more. The rapid data collection methodology profiles fields at a ~20 ha/hour rate at a commercial cost that is comparable to other scanning and sampling services. In addition to generating maps for traditional precision farming practices such as variable seeding and management zones, the new sensors and depth information can assist with soil carbon inventories and soil health initiatives. The CoreScan was evaluated on several fields throughout the USA in conjunction with other Veris scanners. Lab-analyzed samples were collected and correlated with sensor measurements. The granularity of interpolated X-Y data from the CoreScan and the Veris U3 scanner were compared.

Introduction

Proximal sensing of agricultural fields has been widely deployed since the mid 1990's, primarily using soil electrical conductivity (EC) and electromagnetic induction (EM). These scans provide highly detailed maps of soil variations, most commonly variations in soil texture. Because the signal arrays penetrate the soil in a semi-circular pattern based on electrode or coil orientation and distance, some information about the soil profile is obtained (Figure 1). When there is a textural discontinuity, such as a claypan or a sand lens, EC/EM signals can model depth to the discontinuity (Doolittle et al., 1994). One of the limitations to the effectiveness of using EC/EM as

a profiling tool is the lack of profile specificity of the signal. As seen in Figure 1, there is one response for the total profile and ground-truthing is required to provide detailed soil profile information about the drivers of the response. Multiple arrays with unique investigative depths can provide multiple EC/EM profile responses, but do not eliminate the need for additional ground-truthing. For example, a dry soil clay layer within the profile can have a lower EC/EM response and be erroneously interpreted as a coarse soil layer unless profile soil moisture is known.

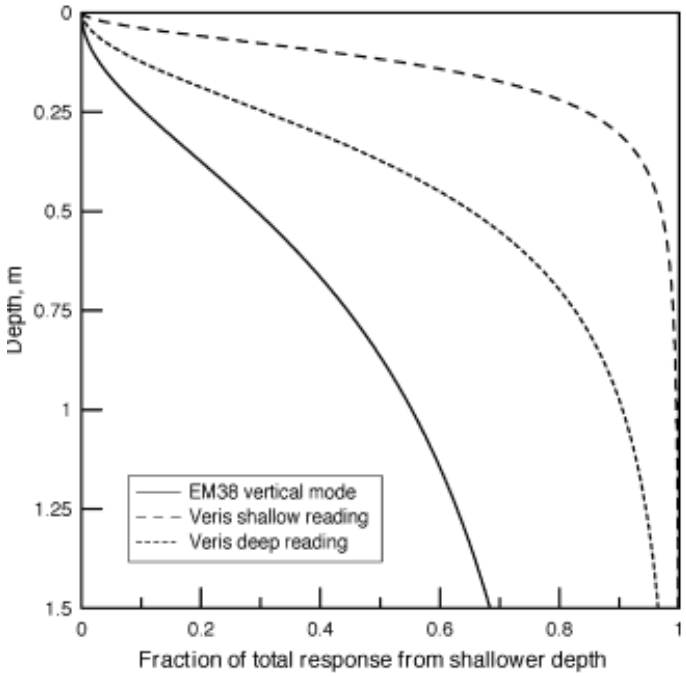

Figure 1. Depth-weighting response of Veris EC and Geonics EM (from Sudduth et al., 2005).

To provide detailed delineations of soil profiles, sensing probes have been developed, including ones with capacitance/moisture sensing that are placed into the soil in season-long, fixed locations to provide soil moisture readings for irrigation management. Due to their cost and complexity these are not proximal sensors that measure profile properties throughout the field. Mobilized sensor probes from various companies have also been developed and commercialized, including Veris Technologies (Pei, et al., 2019), Geoprobe Systems (Christy, et al., 1994), and SIS (Rooney et al., 2002). These technologies, while mobile, are too cumbersome and time-consuming to be affordably inserted at a dense spatial scale. Rather they typically use secondary information such as EC/EM scans, topography maps, or other layers to prescribe a small number of locations for probing. While these instruments provide detailed information at the location where the probe is inserted, there are large areas of fields that are not investigated. For effective management of soil, accurate measurements are needed throughout the profile of: compaction, soil organic carbon (SOC), bulk density, texture, depth of horizons, and water-holding capacity. Reliable information about the entirety of a field's profile will be useful for soil organic carbon inventories, soil health initiatives, tillage practices, site-specific fertilization, yield goals, herbicide effectiveness, irrigation management, and more. To provide high resolution soil profile readings that approach the granularity of surface scanning, an automated multi-sensor probe, the CoreScan, has been developed by Veris Technologies. The CoreScan was operated on more 20 fields in nine US states in conjunction with other Veris scanners. Objectives of this study were to evaluate the accuracy and efficiency of CoreScan using lab analyzed samples, in comparison to surface scanning technology.

Materials and Methods

Sensing Technology

The Veris CoreScan is a hydraulically-activated probe that utilizes four different sensors to characterize the soil profile in 1 cm increments to a depth of 60cm in automatic mode. In manual mode the CoreScan can collect 0-90 cm measurements. The sensors on the CoreScan probe include: Soil EC from a dipole array cone tip, soil reflectance from 660nm and 950nm wavelengths of the visible and near infrared (Vis-NIR) spectrum, capacitance/dielectric sensor, and a load-cell based penetrometer (Figures 2 and 3). These sensors relate to soil texture, SOM, soil moisture, and compaction, respectively. In combination and with lab-analyzed soil samples, they can be used to model: bulk density, horizon depth, profile water-holding capacity, depth to limiting layer, and more.

Figure 2. Veris CoreScan platform--UTV mounting.

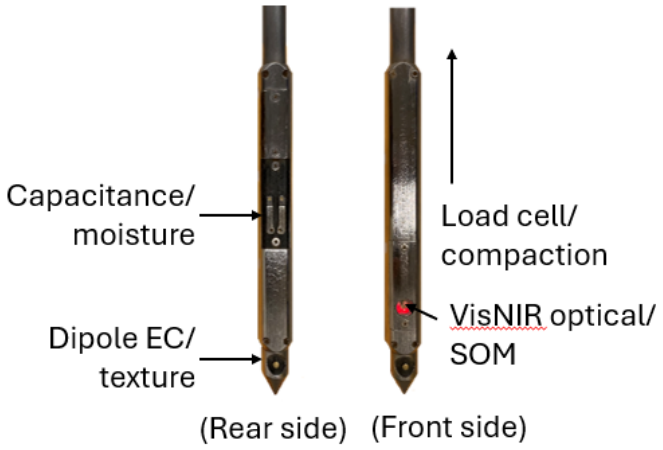

Figure 3. CoreScan sensing technologies.

The CoreScan is automated to efficiently provide closely spaced insertions, typically at least a .4 ha density. Each insertion is controlled and monitored from a V-Sense controller and tablet PC running CoreScan software. To prevent probe damage, the system is designed to stop inserting when insertion force reaches a user-selectable threshold, typically 7.5 MPa for a UTV mounting and 12 MPa for a tractor mounted system. In "continuous" mode the CoreScan senses when the vehicle has stopped and automatically inserts the probe, with no action from the operator. Each cycle takes approximately 50 seconds including travel time between insertions, which provides a capacity of ~25-30 ha/hour on a .4 ha spacing. Profile logs from each sensor can be viewed during data collection and post data collection (Figure 4).

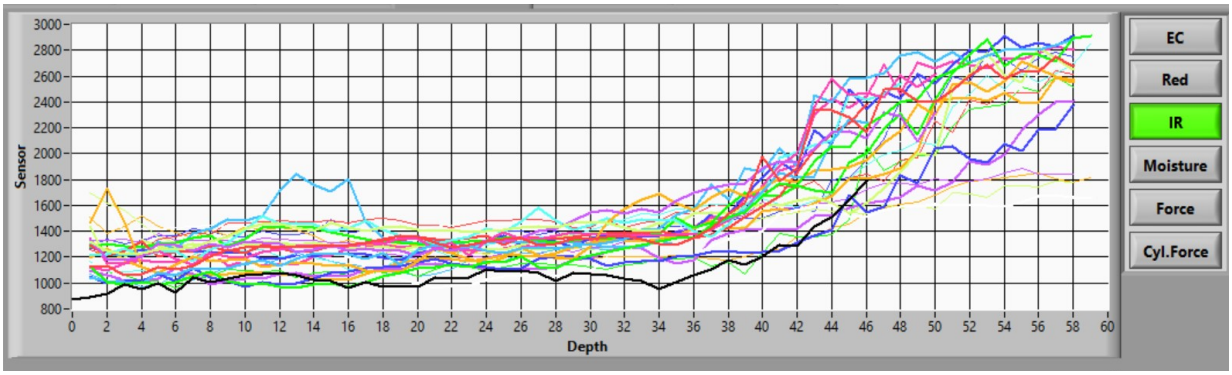

Figure 4. Example of NIR reflectance log.

The Veris U3 scanner includes single Wenner array soil EC sensing using direct contact disc electrodes, with an investigation depth of ~0-60 cm, a 660 nm and 950nm Vis-NIR sensor, and ion-selective pH sensors (Figure 5). EC and optical data is collected at a 1 Hz rate.

Figure 5. Veris U3 system with EC, Vis-NIR, and pH sensing.

Field data collection

In the fall of 2023 and spring of 2024, 21 fields in 9 US cornbelt states were scanned on 15m transects (U3) and sensor-probed (CoreScan) on a .4 ha grid (Figures 6 and 7). 5 fields were located in the central cornbelt (CCB), 8 were in the eastern cornbelt (ECB), 6 were in the northern cornbelt (NCB) and 2 from the western cornbelt (WCB). A minimum of four 0-15 cm calibration samples were collected from each field and 0-60 cm cores were collected from 8 fields. The deeper cores were cut into 0-15, 15-30, and 30-60 cm segments. Samples were lab-analyzed for OM (LOI), CEC (summation), and soil texture (hydrometer). The scanning and probing process was as follows: fields were scanned with the U3 at an average speed of ~10-12 km/hour with a transect omitted every four 15m transects. Upon completing the field, the operator scanned the omitted transects, stopping to automatically insert the CoreScan (and automated pH sensor—data not reported here) every 65m, to a 60cm depth. Insertion speed of the sensor probe was ~6cm/second. Total scanning and sensor probing capacity was ~12 ha/hr.

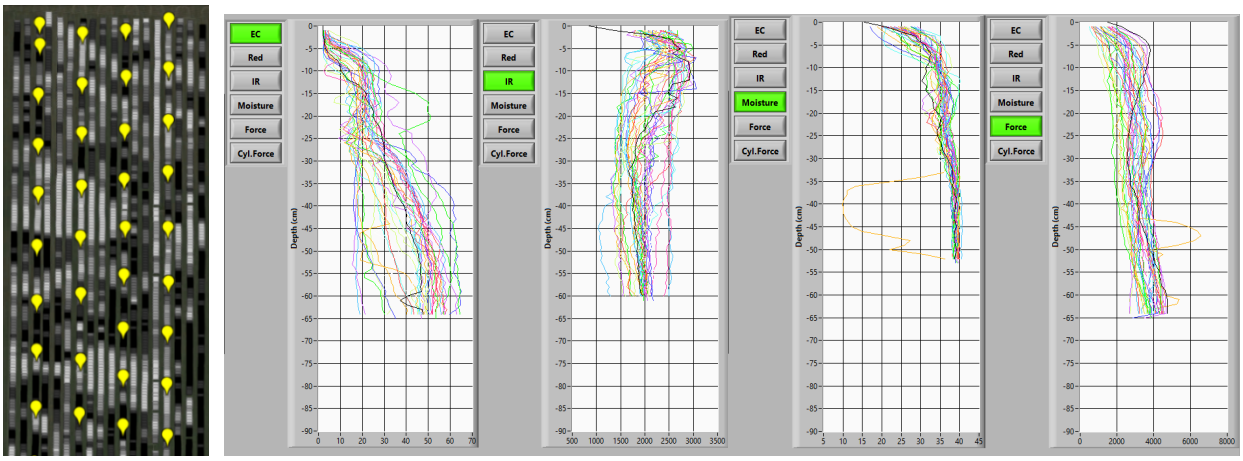

Figure 6. Field ECB1 CoreScan probe locations over 15m soil EC transects from Veris U3.

Figure 7. CoreScan insertion logs for field ECB1.

Results and Discussion

Lab-analyzed soil properties

The lab measurements showed that across all fields the SOM, CEC, and soil texture ranged widely, although variations within many of the fields were low (Table 1). Both sensing devices were able to perform well in soil ranging from 8-80% sand and 8-56% clay, and from .08-7.2% OM.

Table 1. Descriptive statistics of soil OM and CEC for 159 sample points; for soil texture 127 sample points

		OM				CEC				Sand				Clay				Silt			
Field	*N*	*Min*	*Max*	*SD*	*Avg*	*Min*	*Max*	*SD*	*Avg*	*Min*	*Max*	*SD*	*Avg*	*Min*	*Max*	*SD*	*Avg*	*Min*	*Max*	*SD*	*Avg*
CCB1	10	2.5	6.1	1.1	3.4	11.1	19.5	2.6	14.4	38	54	5.7	46.7	20	28	2.5	24.5	22	38	5.4	29.0
CCB2	13	2.6	4.3	0.5	3.6	8.2	18.7	1.4	16.6	16	42	6.9	22.9	28	32	1.0	29.8	16	54	12.0	47.0
CCB3	7	3.1	7.2	1.6	4.3	11	26.1	5.7	16.6	18	26	2.8	20.3	24	36	4.6	31.1	44	54	4.3	48.7
CCB4	8	3.5	4.8	0.4	3.9	14.8	20.5	1.8	17.9	10	14	1.7	11.8	26	34	2.7	30.0	56	62	2.3	58.5
CCB5	4	3.1	4.4	0.6	3.6	13.5	15.4	0.8	14.5	12	22	4.4	16.5	20	26	2.6	23.0	56	62	3.0	60.0
ECB1	17	3.1	5	0.5	3.8	14	17.2	0.9	15.5	8	18	2.6	11.4	28	36	2.3	30.1	50	62	3.6	58.0
ECB2	6	1.7	3.6	0.8	2.5	8.2	18.1	3.8	12.9	16	58	15.4	34.7	18	48	12.1	30.3	24	40	5.8	35.0
ECB3	5	2.3	3.8	0.6	3.0	10.5	20.9	4.8	16.4	20	28	3.3	24.4	34	40	2.3	36.8	38	40	1.1	39.0
ECB4	4	2.3	3.7	0.6	3.2	10.8	16	2.1	14.3	26	28	1.2	27.0	30	36	2.6	33.0	38	42	1.6	40.0
ECB5	4	2.2	3.3	0.5	2.9	8.6	20.9	5.2	13.8	26	34	3.4	29.0	28	34	2.5	31.0	34	44	4.3	39.6
ECB6	5	1.8	4.1	1.0	2.9	10.2	18.4	3.7	15.0	20	44	9.7	28.0	20	32	4.7	28.0	36	52	6.3	44.2
ECB7	4	2	4.4	1.1	3.0	9.2	19.9	4.4	14.3	20	36	7.2	25.5	24	36	5.3	31.0	34	54	8.2	43.6
ECB8	5	1.1	1.7	0.2	1.4	3.5	5.5	0.8	4.3	74	80	3.0	77.2	8	12	1.7	9.6	10	16	2.3	13.2
NCB1	7	1.3	2.8	0.6	1.9	5.9	12.2	2.4	8.9	36	68	13.9	50.9	10	20	4.3	15.1	22	34	10.0	34.0
NCB2	7	3.1	5.2	0.8	3.8	9.4	15.1	2.1	11.4	22	30	2.6	25.3	18	28	3.6	21.6	50	56	2.0	53.1
NCB3	4	1.9	4.1	0.9	2.9	11.7	15.4	1.5	13.7	NA	NA	NA	NA	NA	NA	NA	NA	NA	NA	NA	NA
NCB4	4	0.8	1.2	0.2	1.0	3.4	4.8	0.7	4.1	NA	NA	NA	NA	NA	NA	NA	NA	NA	NA	NA	NA
NCB5	4	3.2	4.4	0.5	3.9	12.8	17.2	1.8	15.0	18	32	6.5	22.0	22	40	8.3	32.0	40	58	8.2	46.0
NCB6	4	2.2	2.8	0.3	2.5	11.6	14.7	1.4	12.7	24	28	1.9	25.5	24	26	1.2	25.0	42	58	1.9	49.4
WCB1	12	2.6	4.1	0.4	3.1	13.1	23.6	3.0	16.4	18	22	1.0	20.7	20	56	10.7	27.7	48	58	3.0	52.0
WCB2	25	1.9	2.8	0.2	2.3	19.2	32.4	3.8	24.9	NA	NA	NA	NA	NA	NA	NA	NA	NA	NA	NA	NA

Visual inspection of core samples, lab-analyzed results, and accompanying logs exhibit proper relationships: areas of the profile that are visibly darker have higher OM and decreased optical reflectance, and areas with higher clay content have higher soil EC (Figure 8 a-b).

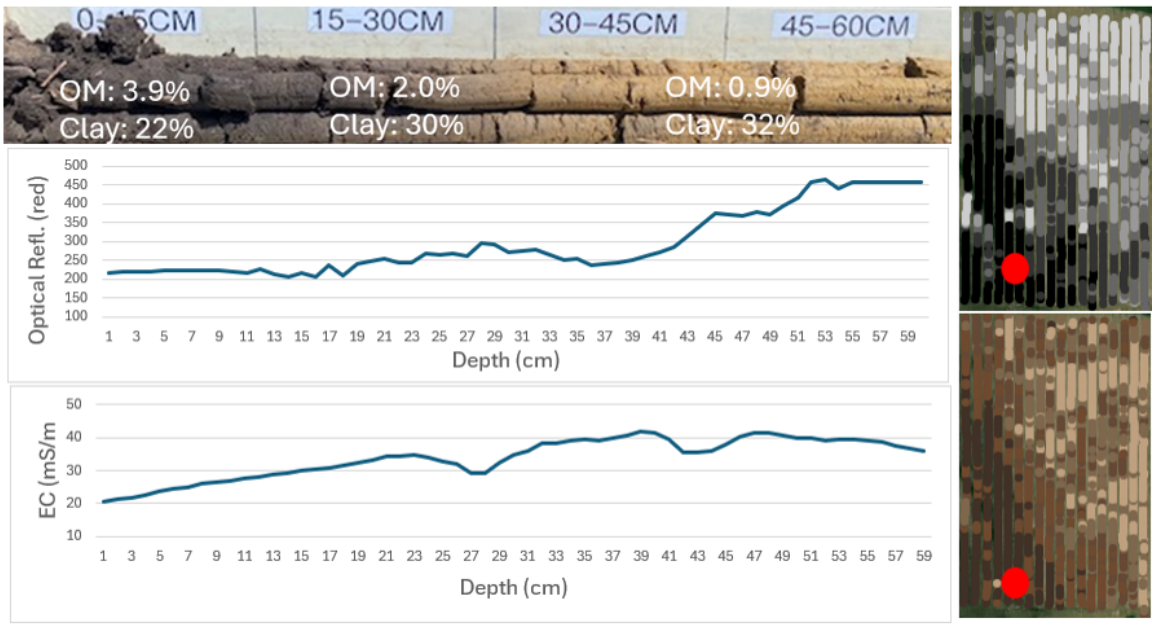

Figure 8a. Soil core and CoreScan log from southwest area of Field CCB1 (U3 scan).

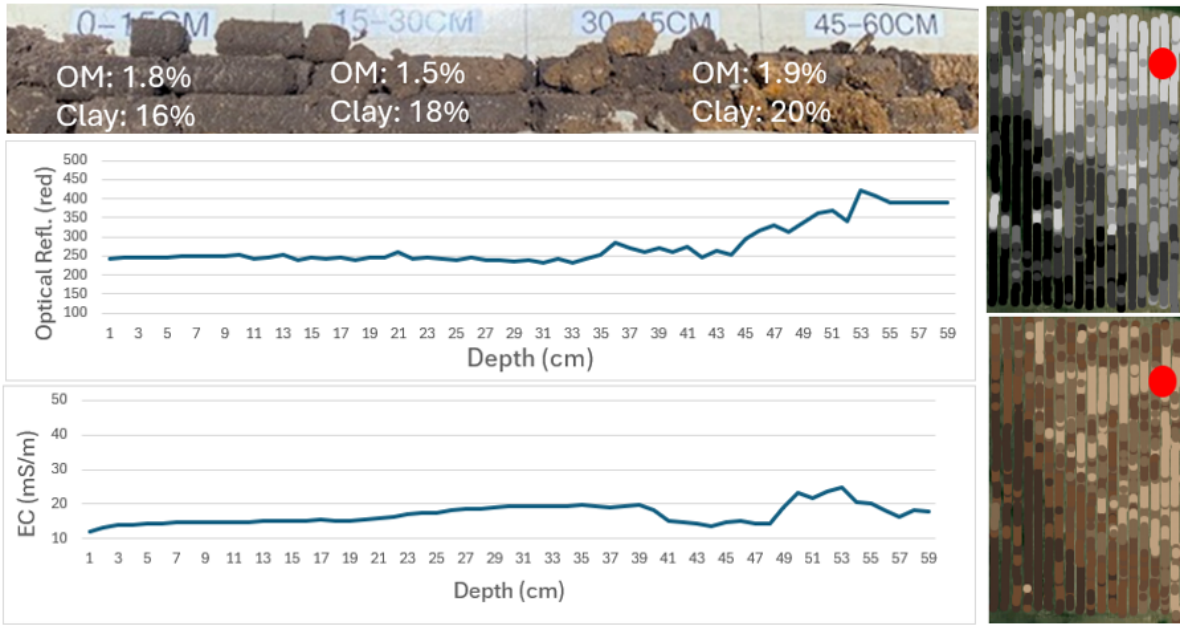

Figure 8b. Soil core and CoreScan log from northeast area of Field CCB1 (U3 scan).

To evaluate sensor performance and develop calibrations, lab samples and co-located soil sensor readings were matched, and simple bivariate regression was performed, and the strongest correlations reported (Tables 2 and 3). As would be expected based on typical relationships between soil attributes and EC and optical sensing, CEC and clay content were positively correlated with EC, while OM was inversely correlated with red and IR reflectance measurements using both instruments.

Table 2. OM and CEC calibration set correlation coefficients (R), root mean square errors (RMSE), and ratio of performance to deviation (RPD: std deviation/RMSE); sensor used for calibration

	OM: Veris CoreScan				OM: Veris U3				CEC: Veris CoreScan				CEC: Veris U3			
Field ID	Sensor	R	RMSE	RPD	Sensor	R	RMSE	RPD	Sensor	R	RMSE	RPD	Sensor	R	RMSE	RPD
CCB1	IR 0-60	-0.91	0.44	2.55	IR	-0.62	0.83	1.35	IR_45	-0.92	1.02	2.75	EC 0-2	0.93	1.00	2.80
CCB2	Red_45	-0.86	0.23	2.03	Red	-0.71	0.30	1.49	EC_15	0.33	1.17	1.10	IR	0.32	1.22	1.10
CCB3	IR_30	-0.96	0.45	3.90	IR	-0.95	0.52	3.36	EC_30	0.96	1.37	3.95	EC 0-2	0.83	2.80	1.93
CCB4	EC_15	-0.49	0.38	1.22	Red	-0.78	0.27	1.72	EC 0-60	0.88	0.79	2.23	EC 0-2	0.65	1.25	1.41
CCB5	IR_60	-0.89	0.23	2.54	Red	-0.70	0.35	1.62	EC_30	-0.88	0.33	2.42	IR	-0.76	0.45	1.76
ECB1	EC_15	-0.72	0.33	1.49	EC 0-2	-0.63	0.37	1.33	Moisture	0.44	0.84	1.14	IR	-0.76	0.60	1.59
ECB2	IR_30	-0.97	0.18	4.54	EC 0-2	0.49	0.67	1.25	IR 0-60	-0.92	1.32	2.88	EC 0-2	0.63	2.69	1.41
ECB3	IR_30	-0.98	0.12	5.46	IR	-0.81	0.33	1.90	EC_15	0.84	2.36	2.04	EC 0-2	0.95	1.31	3.67
ECB4	IR_15	-0.94	0.19	3.26	Red	-0.93	0.20	3.09	IR_15	-0.99	0.08	30.6	EC 0-2	0.81	1.19	1.99
ECB5	IR_15	-0.85	0.25	2.17	Red	-0.97	0.12	4.61	EC_15	0.90	1.99	2.63	EC 0-2	0.95	1.46	3.58
ECB6	IR_30	-0.80	0.51	1.88	IR	-0.98	0.18	5.33	EC_15	0.86	1.71	2.16	EC 0-2	0.68	2.44	1.52
ECB7	Red_30	-0.99	0.11	9.60	Red	-0.88	0.44	2.45	EC_15	0.84	2.09	2.12	EC 0-2	0.97	0.97	4.56
ECB8	IR_45	-0.89	0.10	2.52	EC 0-2	0.56	0.18	1.35	EC_30	0.99	0.12	8.21	EC 0-2	0.89	0.34	2.46
NCB1	EC_15	0.99	0.08	8.25	IR	-0.92	0.21	2.75	EC_15	0.94	0.87	3.30	EC 0-2	0.83	1.40	1.92
NCB2	IR_30	-0.90	0.30	2.49	Red	-0.99	0.10	7.43	Red_30	-0.90	0.85	2.50	EC 0-2	0.92	0.76	2.79
NCB3	IR_60	-0.83	0.44	2.06	Red	-0.95	0.25	3.62	Red_30	-0.87	0.64	2.38	Red	-0.99	0.10	14.8
NCB4	Red_45	0.89	0.07	2.51	Red	-0.46	0.13	1.30	IR_30	-0.93	0.21	3.22	EC 0-2	0.77	0.36	1.82
NCB5	IR_15	-0.99	0.04	11.85	IR	-0.98	0.09	5.28	EC_15	0.92	0.63	2.94	EC 0-2	0.92	0.64	2.90
NCB6	Red_15	-0.92	0.09	2.94	EC 0-2	-0.96	0.06	4.05	EC_45	-0.83	0.69	2.07	EC 0-2	-0.82	0.71	2.01
WCB1	IR_30	-0.69	0.34	1.46	EC 0-2	0.70	0.31	1.47	EC_30	0.48	2.97	1.20	EC 0-2	0.77	2.04	1.64
WCB2	EC 0-15	-0.46	0.19	1.15	EC 0-2	-0.60	0.17	1.27	EC 15-30	0.48	2.81	1.16	EC 0-2	0.64	2.46	1.32

Table 3. Soil texture calibration set correlation coefficients (R), root mean square errors (RMSE), and ratio of performance to deviation (RPD)

	Clay: Veris CoreScan				Clay: Veris U3				Sand: Veris CoreScan				Sand: Veris U3				Silt: Veris CoreScan				Silt: Veris U3			
Field ID	Sensor	R	RMSE	RPD	Sensor	R	RMSE	RPD	Sensor	R	RMSE	RPD	Sensor	R	RMSE	RPD	Sensor	R	RMSE	RPD	Sensor	R	RMSE	RPD
CCB1	EC_15	0.68	1.7	1.4	EC 0-2	0.57	1.9	1.3	Force	0.75	3.7	1.6	EC 0-2	-0.49	4.8	1.2	Moist	0.62	4.0	1.3	Red	-0.49	4.4	1.2
CCB2	Cyl Force	0.35	1.0	1.1	EC 0-2	0.17	1.1	1.1	Force	-0.50	10.4	1.2	EC 0-2	0.41	10.6	1.1	Force	0.51	10.3	1.2	EC 0-2	-0.43	10.4	1.2
CCB3	Force	0.74	3.1	1.6	EC 0-2	0.13	4.6	1.1	Force	-0.73	1.7	1.6	Red	-0.72	1.7	1.6	Force	-0.54	3.3	1.3	IR	0.39	3.6	1.2
CCB4	EC_15	0.88	1.3	2.2	EC 0-2	0.82	1.6	1.9	EC_15	-0.61	1.1	1.3	Red	-0.81	0.8	1.8	EC_45	-0.90	1.0	2.4	EC 0-2	-0.90	1.0	2.4
CCB5	EC 0-60	0.94	0.8	3.3	EC 0-2	0.91	0.9	2.8	EC 0-60	-0.94	1.3	3.4	EC 0-2	-0.93	1.4	3.1	Red_45	0.99	0.4	6.7	EC 0-2	0.59	2.1	1.4
ECB1	EC_60	-0.57	1.8	1.3	EC 0-2	-0.42	2.0	1.1	Moist	0.67	1.8	1.4	EC 0-2	-0.59	2.0	1.3	Red_60	0.78	2.2	1.7	EC 0-2	0.67	2.6	1.4
ECB2	Moist	0.98	2.4	5.1	EC 0-2	0.76	7.2	1.7	Moist	-0.98	2.7	5.7	EC 0-2	-0.93	5.1	3.0	EC_45	0.98	1.0	5.9	EC 0-2	0.91	2.2	2.6
ECB3	EC_15	0.69	1.5	1.6	EC 0-2	0.64	1.6	1.5	Red_45	0.92	1.2	2.8	EC 0-2	-0.65	2.2	1.5	Red_45	-0.99	0.2	7.1	EC 0-2	0.64	0.8	1.4
ECB4	Moist	-0.95	0.7	3.8	Red	-0.91	0.9	2.7	Red_45	0.87	0.5	2.3	Red	0.63	0.8	1.5	IR_15	0.83	0.8	2.0	Red	0.99	0.2	8.5
ECB5	EC_30	0.88	1.1	2.5	IR	-0.97	0.6	4.4	EC_60	0.84	1.6	2.1	EC 0-2	0.58	2.4	1.4	Moist	-0.98	0.7	6.3	EC 0-2	-0.93	1.4	3.1
ECB6	EC_15	0.84	2.3	2.0	EC 0-2	0.68	3.1	1.5	EC_30	-0.94	3.0	3.2	EC 0-2	-0.35	8.1	1.2	EC_30	0.99	0.5	12.5	Red	0.57	4.6	1.4
ECB7	EC_15	-0.89	2.1	2.5	EC 0-2	-0.41	4.2	1.3	Force	0.99	1.0	7.4	EC 0-2	-0.81	3.6	2.0	IR 0-60	0.99	0.2	43.5	EC 0-2	0.98	1.6	5.3
ECB8	Force	0.98	0.3	6.4	EC 0-2	-0.62	1.2	1.4	IR_30	0.96	0.8	4.1	IR	-0.31	2.6	1.2	IR_30	-0.95	0.7	3.7	EC 0-2	0.39	1.9	1.2
NCB1	EC_30	0.96	1.3	3.9	EC 0-2	0.91	1.8	2.7	EC_30	-0.95	4.3	3.5	EC 0-2	-0.91	5.6	2.7	EC_30	0.94	3.0	3.4	EC 0-2	0.91	3.8	2.6
NCB2	IR_30	-0.86	1.7	2.1	EC 0-2	0.93	1.2	3.0	Moist	-0.77	1.6	1.7	EC 0-2	-0.68	1.8	1.5	Red	0.85	1.0	2.0	EC 0-2	-0.78	1.1	1.7
NCB5	Moist	0.99	0.9	9.0	Red	-0.97	1.9	4.4	EC_30	-0.98	1.1	6.1	EC 0-2	-0.94	2.1	3.3	IR_30	0.95	2.2	3.6	IR	0.87	3.5	2.3
NCB6	IR_15	0.99	0.1	8.9	EC 0-2	0.68	0.7	1.6	EC_45	-0.91	0.7	2.8	EC 0-2	-0.85	0.9	2.2	EC_15	0.97	0.4	4.9	EC 0-2	0.44	1.5	1.3
WCB1	Cyl Force	-0.54	8.6	1.3	EC 0-2	0.43	8.5	1.2	EC_45	-0.57	1.1	1.3	EC 0-2	-0.42	1.1	1.2	IR_30	0.56	2.6	1.3	EC 0-2	-0.67	2.1	1.4

Soil depth indicators

The depth to color change was estimated by finding the first significant change from darker to lighter soil which was 10% or greater from the starting optical response in the sensed profile. To programmatically determine this change in optical response, a polynomial line was fitted over the sensor data points and the first derivative of this line was calculated. The first derivative represents the slope at any point on a line. The point with the maximum slope represents the largest change in sensor response from darker to lighter soil (Figure 9). The optical response from this inflection point and 3cm deeper was averaged and compared to the average optical response from the top 8-16cm. If this represented a 10% change then it was recorded as the depth to color change. If not, the depth to color change was recorded as the maximum insertion depth.

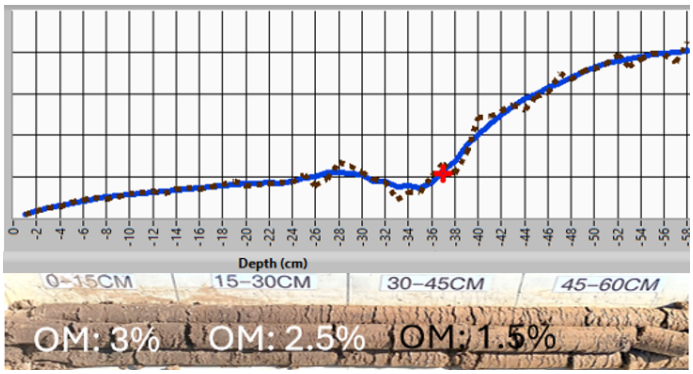

Figure 9. Derived depth to color change on Field CCB1 with core photo and lab OM results.

Soil moisture measurements

The CoreScan's suite of soil sensors provides a temporal measurement of soil moisture at the time of probing, and the soil texture and the OM sensors provide the inputs needed to model available water holding capacity (AWHC) using the SPAW model (Saxton and Rawls, 2006) (Table 4). Soil moisture was measured on each insertion with a 100 MHz capacitance sensor embedded in the CoreScan probe rod. Fields probed in the fall had overall slightly less moisture and more variable moisture than the spring-probed fields, as could be expected following cropping versus spring recharge (Table 4a). Available water-holding capacity was modeled with the SPAW model which uses soil texture and OM to estimate AWHC. The AWHC of the fields and the profiles varied widely based on sand and clay content (Table 4b). The temporal moisture measurements were modestly correlated with AWHC (.29 R^2).

Table 4a-b. 4a. Sensor-measured soil moisture. 4b. Modeled available water-holding capacity

		0-60 cm measured moisture (gravimetric%)						0-60 cm AWHC (cm per meter)			
Field	N	Min	Max	SD	Avg	CV	Season	Min	Max	SD	Avg
CCB1	26	31.6	38.7	1.7	35.3	0.05	spring	12.2	15.3	0.71	13.1
CCB2	36	32.5	36.5	0.9	34.9	0.03	spring	15.3	17.0	0.40	16.0
CCB3	19	34.9	39.4	1.3	37.1	0.04	fall	15.9	19.0	0.91	17.2
CCB4	19	36.6	39.4	0.7	37.6	0.02	spring	17.3	19.1	0.50	18.0
CCB5	13	33.7	36.7	0.6	35.7	0.02	fall	17.7	19.8	0.77	18.8
ECB1	37	36	37.9	0.5	37	0.01	spring	17.2	18.4	0.32	17.8
ECB2	16	24.3	36.4	3.3	32.9	0.10	fall	10.9	15.2	1.10	13.2
ECB3	38	34.1	38.5	1	36	0.03	fall	14.3	14.7	0.08	14.5
ECB4	8	25.1	27.9	0.8	26.5	0.03	fall	14.6	14.9	0.08	14.7
ECB5	23	31.4	37.8	1.5	35.7	0.04	fall	14.0	15.5	0.42	14.7
ECB6	37	24	27.8	0.9	26.2	0.03	fall	12.0	16.1	0.96	13.7
ECB7	9	18.7	37.2	6.9	31.5	0.22	fall	13.4	20.1	2.41	16.3
ECB8	36	20.1	23.4	0.8	21.7	0.04	fall	5.9	7.3	0.25	6.4
NCB1	17	32	36.3	1.5	33.8	0.04	spring	6.2	15.7	2.01	11.0
NCB2	17	35.5	39.5	1.1	36.9	0.03	spring	17.2	17.5	0.08	17.4
NCB3	28	30.1	41.3	2.9	34.4	0.08	fall	NA	NA	NA	NA
NCB4	134	19.5	32.8	2.5	27.4	0.09	spring	NA	NA	NA	NA
NCB5	18	33.4	37.2	1.1	35.5	0.03	fall	15.2	16.9	0.42	16.4
NCB6	17	31.5	36.4	1.2	34.3	0.03	fall	16.0	16.4	0.13	16.3
WCB1	32	17.6	23.9	1.6	21	0.08	spring	15.1	19.2	0.86	16.5
WCB2	25	27.6	40.9	3.1	37.7	0.08	spring	NA	NA	NA	NA

Soil compaction measurements

Soil compaction is sometimes referred to as the hidden yield robber—hidden because it is within the profile and not easily detected especially at a dense spatial scale, and a yield robber due to the significantly negative impact it can have on crop yield. It is frequently listed as a soil health indicator. Various compaction levels have been proposed as harmful to root growth, including 1.25 MPa (Bennie and Burger, 1980). Whether a compaction level is harmful varies with soil texture (USDA-NRCS, 2008). Ken Ferrie, agronomist for Farm Journal magazine, reports diminished yields may be due to sudden density changes in the profile, more than gradually increasing density to a high level of compaction (Smith, 2023). Other factors make this soil condition difficult to assess: soil moisture affects penetrometer readings with increased resistance as soil dries, and compaction is highly spatially variable, caused by wheel traffic, by tillage, and by soil texture interfaces. The CoreScan sensors are uniquely positioned to deal with these complexities due to the accompanying moisture and texture sensing, its penetrometer controlled insertion speed, and automation that allows dense investigations.

A common compaction tool used in the USA is an analog hand probe with a dial showing green/yellow/red for various compaction levels. Converting that dial to the penetrometer tip size of the CoreScan, the red/danger level would be at ~2750 KPa. A higher compaction level was also considered—4100 Kpa.

Insertion forces were measured in 1 cm increments on each insertion with a load cell sensor embedded in the head of the CoreScan probe. Fields probed in the fall had 40% higher insertion force and exhibited 50% greater variability than the spring-probed fields, as could be expected for fall versus spring conditions, and follows a similar pattern as moisture (Table 5a). 12 MPa is the maximum probe force before possible damage, so the automation was set to discontinue inserting when that force was reached, either due to a stone or extremely compacted layer. Only 2% of the insertions experienced 12 MPa. Depth to compacted layer, as defined by the depth in the soil

profile where 2750 and/or 4100 KPa are reached reveals some interesting phenomena: 1) insertion forces in the spring averaged 40% less than the fall probing, demonstrating the need accounting for soil moisture; 2) all spring fields other than WCB1 field that was in drought conditions had at least one insertion that reached the 45 cm before 4100 Kpa, and 3) all fields had at least one insertion that reached the 2750 threshold at or very near the surface (Table 5b).

Tables 5a-b. Measured insertion forces in 0-60 cm and depths to compaction

	Table 5a. Avg. insertion forces 0-60 cm (Kpa)							Table 5b. Depth (cm) to 4100				Depth(cm) to 2750 Kpa			
Field	*N*	*Min*	*Max*	*SD*	*Avg*	*Season*	*>12 Mpa*	*Min*	*Max*	*Avg*	*SD*	*Min*	*Max*	*Avg*	*SD*
CCB1	26	2683	4121	412	3293	spring	1	14	64	43	14.3	3	27	10	4.6
CCB2	36	2645	4613	442	3624	spring	0	9	64	28	12.8	1	27	8	5.3
CCB3	19	2855	4411	542	3559	fall	0	11	64	35	16.2	1	15	8	3.6
CCB4	19	2209	3575	326	2963	spring	0	17	64	54	21.8	7	18	14	3.0
CCB5	13	2985	5199	603	3875	fall	1	14	63	27	4.3	6	16	10	3.3
ECB1	37	2084	3983	450	3123	spring	0	14	64	55	21.3	1	51	15	15.1
ECB2	16	3556	9314	1444	6103	fall	3	3	38	17	7.6	1	25	9	6.6
ECB3	38	2540	5230	617	3807	fall	0	12	42	25	7.5	5	27	12	5.3
ECB4	8	2400	5043	878	3571	fall	0	10	40	20	6.7	3	17	9	6.3
ECB5	23	4249	8627	1036	5528	fall	1	6	17	12	2.9	1	10	5	2.5
ECB6	37	2767	5890	777	4171	fall	2	3	36	11	2.8	1	9	4	2.1
ECB7	9	4708	8542	1631	6042	fall	2	1	19	11	4.4	1	7	4	2.2
ECB8	36	2422	4606	538	3286	fall	0	7	33	18	5.4	1	20	9	5.8
NCB1	17	1764	4000	491	2422	spring	1	10	64	59	21.2	4	63	36	24.7
NCB2	17	2060	4009	516	2605	spring	0	1	64	35	23.2	1	54	16	17.1
NCB3	28	3472	7916	1086	5693	fall	0	6	57	20	12.5	1	20	7	4.8
NCB4	134	2690	6715	913	4629	spring	3	12	49	24	5.8	5	34	20	5.9
NCB5	18	2598	4178	391	3321	fall	0	14	63	43	17.0	7	18	13	3.1
NCB6	17	2290	4159	538	3371	fall	0	1	43	30	11.4	1	24	13	5.7
WCB1	32	1639	3683	529	2387	spring	0	22	38	36	7.1	11	37	28	9.1
WCB2	25	2101	3998	480	2927	spring	0	21	60	50	12.7	7	59	24	14.5

Georeferenced depth to compaction measurements on each field shown in Table 5b can be generated as a tillage script prescribing the precise depths that are needed to remove the compaction layer (Figure 10.)

Figure 10. Depth to 4100 Kpa compaction layer

Additionally, viewing insertion force logs from each field exposes differences in soil density signatures. Some fields had evidence of historical density layers at the ~20 cm plow pan depth, while some fields had more gradually changing density, especially those in long term no-till (Figures 11 and 12).

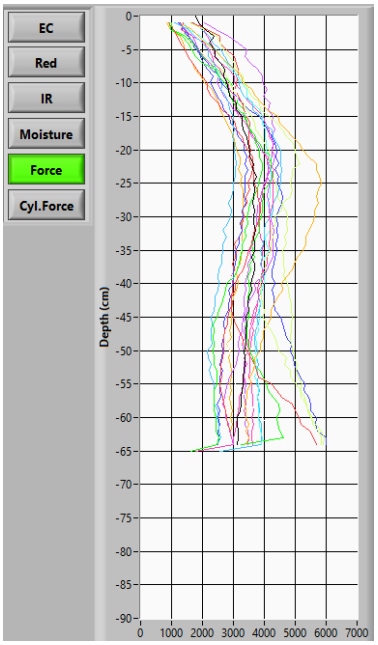

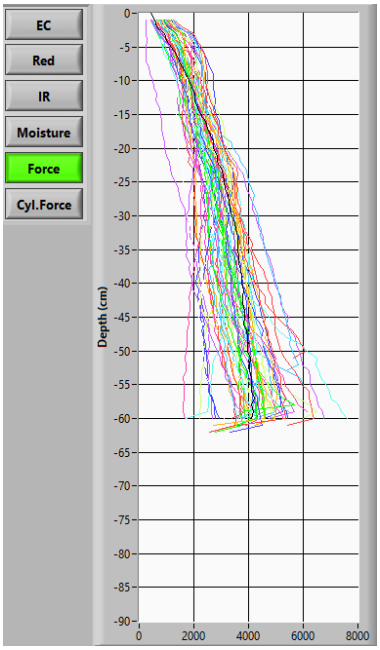

Figures 11. Insertion force from conventionally tilled field, CCB3.

Figure 12. Insertion force log from long-term no-till field, WCB2

Resolution: .4 ha probing versus 15m scanning

Because all fields in this project were scanned on 15m transects and probed on .4 ha grids with similar sensors (EC and optical), those data from each device can be interpolated and compared. It is apparent in viewing maps that a .4 ha spacing on some fields adequately defines the variability, due to its spatial structure (Figure 13).

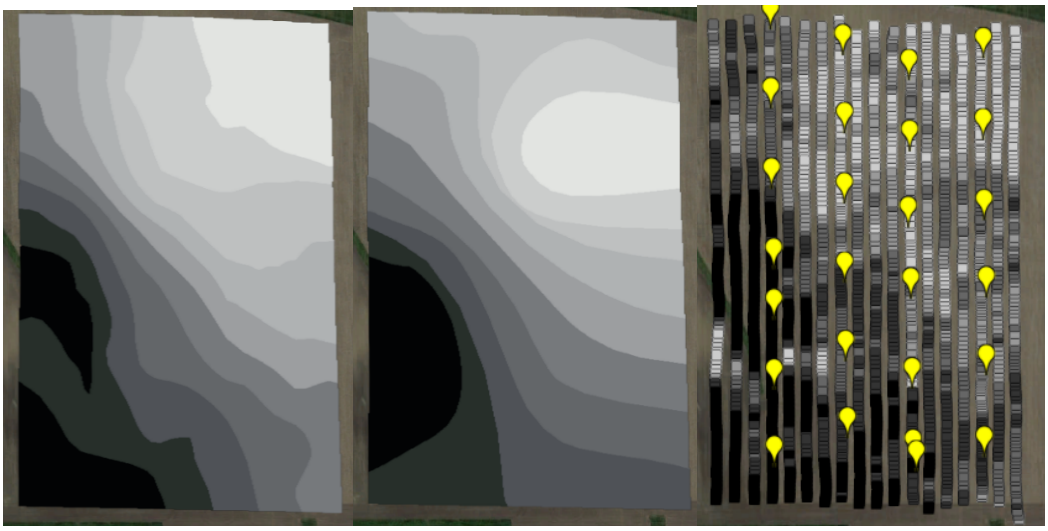

Figure 13. Contoured EC maps from field CCB1 from U3 15m transects (left) and .4 ha CoreScan (center). Probe points overlaid on transect data (right).

Other fields exhibit a markedly different appearance between the two maps and it is evident that the 15m transects are needed on some fields to capture variability (Figure 14).

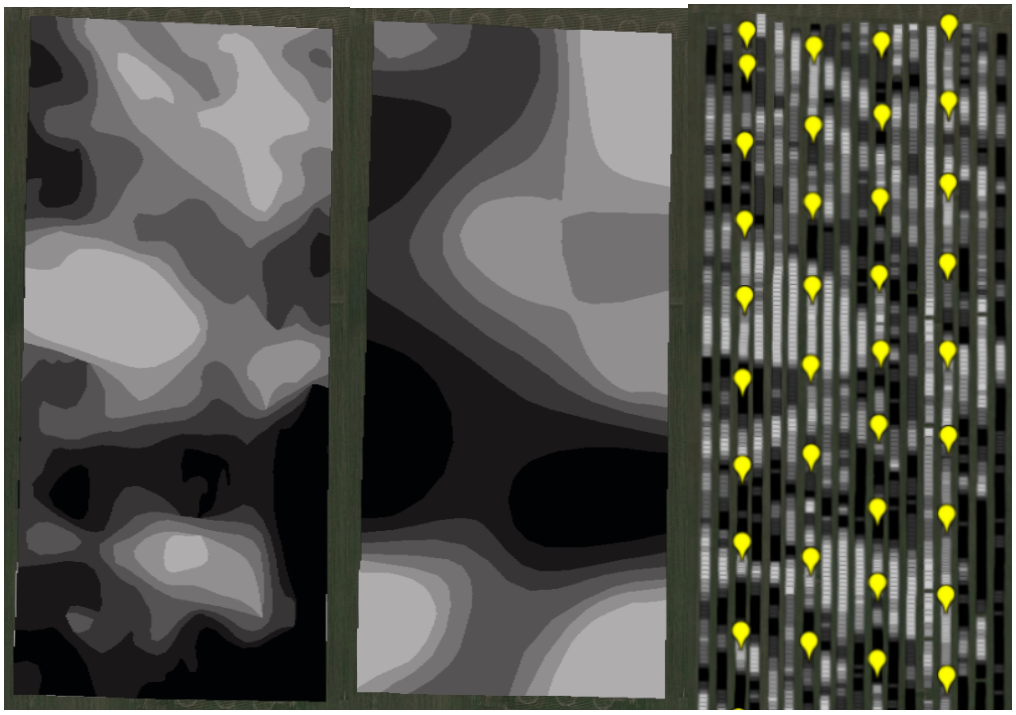

Figure 14. Contoured EC maps from field ECB1 using from U3 15m transects (left) and .4 ha CoreScan (center). Probe points overlaid on transect data (right).

In an attempt to quantify the difference in field coverage detail of the CoreScan .4 ha grid vs. the 15m transects of the U3 on all studied fields, both datasets were interpolated and gridded into a matching 10m x 10m raster and compared. The U3 was considered as the baseline and the correlation with the CoreScan evaluated. The results suggest that on about 1/3 of the fields the .4 ha grid is likely adequate, similar to Figure 13 above, and on 1/3 the 15m transects are clearly superior similar to Figure 14, with the other third of the fields questionable. This subject will be investigated further, and likely usage of both systems will continue and, in many cases, will be used in conjunction with each other. One device provides significantly more XY granularity and the other has more sensors to generate detailed -Z variability and considerable XY information. Some considerations as to which platform to use where and when include: the variability that matters most--the soil profile or field XY, or both; the application of the data—what scale will be needed, for example 40m wide spray booms vs. 3m wide planters; and crop and input values—vineyards vs wheat fields. Another alternative is to reduce the CoreScan grid size, perhaps down to .25 ha grids, which could be accomplished and yet maintain 15 ha/hour rate.

Future Research

This project created a large amount of data and yielded insights about fields, profiles, and sensors. It also generated many questions and opportunities for future research, including investigating how these sensors can improve soil carbon and bulk density measurements, address soil health concerns, integrate management zones and other ancillary layers such as topography, yield maps and remote sensing. Machine learning techniques are needed, especially to exploit the interactions between sensors to better derive profile information on horizon depths and locations and causes of soil compaction.

Conclusions

This was an extensive project spanning 21 fields across 9 US states over two seasons to evaluate the new CoreScan technology, comparing lab-analyzed samples and the U3 scanning sensors to the CoreScan measurements. Correlation to measured physical and biological soil properties demonstrated acceptable EC and optical sensor accuracy, with overall RPD's >2 and with low prediction errors. The EC and optical sensors on each system were comparable both in correlation between each other (other than spatial resolution) and to lab results. Both systems demonstrated operational suitability, in terms of efficient data collection, automation, and equipment durability. More than 50% of the fields were measured in the fall after cropping and in a drier than normal year, yet insertion forces were well within the capacity of the probe, with only 2% exceeding the force rating, and all fields were able to be fully covered. The CoreScan demonstrated that it can perform near lab-quality OM, CEC, and soil texture measurements, collect soil moisture and compaction data at 1 cm resolution from 0-60 cm. Initial investigations into deriving water-holding capacity, depth to compacted layers, depth to color and texture changes were successfully conducted on all fields.

References

Bennie, A. T. P., and Burger, R. du T. (1980). The effect of soil compaction on root growth and nutrient uptake by maize. Proc. 9th National Congress of Soil Science Society of SA Tech Comm 174: 2-9.

Christy, C.D., T.M. Christy, and V. Witting. 1994. A percussion probing tool for the direct sensing of soil conductivity. In: Proceedings of the 8th National Outdoor Action Conference, 381–394. Westerville, Ohio: National Ground Water Association.

Doolittle, J. A., Sudduth, K.A., Kitchen, N.R., Indorante, S.J. 1994 Estimating Depth to Claypans Using Electromagnetic Induction Methods. Journal of Soil and Water Conservation, 49, 572-575.

Rooney, D.J., M. Dudka, M. Cheyne, and J.R. Samuelson. 2002. The Soil Information System. ASAE Annual Conference Proceedings.

Saxton, K. E., and W. J. Rawls. 2006. Soil Water Characteristic Estimates by Texture and Organic Matter for Hydrologic Solutions. Soil Sci. Soc. Am. J. 70:1569-1578.

Smith, D., Nov 17, (2023) Do You Have Soil Compaction and Density Changes That Impede Roots and Water? Here's How to Find Out | AgWeb

Sudduth, K.A., Kitchen, N.R., Wiebold, W.J., Batchelor, W.D., Bollero, G.A., Bullock, D.G., Clay, D.E., Palm, H.L., Pierce, F.J., Schuler, R.T., Thelen, K.D. 2005. Relating apparent electrical conductivity to soil properties across the north-central USA. Computers and Electronics in Agriculture 46, 263–283.

USDA-NRCS. 2008. Soil Quality Indicators - Bulk Density.

Xiaoshuai, P., Sudduth, K.A., Veum, K.S., Li, M. 2019. Improving In-Situ Estimation of Soil Profile Properties Using a Multi-Sensor Probe Sensors (Basel). 2019 Mar; 19(5): 1011. Published online 2019 Feb 27.